doi:10.3788/gzxb20174604.0413001

Cu^{2+}离子注入的石英光波导的特性研究

刘秀红,韩海燕,朱巧芬,黄艳宾,董昭
(河北工程大学 数理科学与工程学院,河北 邯郸 056038)

摘　要:利用 Cu^{2+} 离子注入的方式在熔融石英和石英晶体上分别制备了平面光波导结构.通过棱镜耦合实验测试了两种光波导的导模特性,结果表明:在同样的注入条件下熔融石英上形成了增加型的光波导结构,而石英晶体上形成了位垒型的光波导结构.研究了退火温度对两种光波导导模折射率的影响,熔融石英光波导中导模的折射率随着退火温度的升高而降低,而石英晶体光波导中导模的折射率随着退火温度的升高先增加后降低.为了进一步分析离子注入两种材料形成光波导的微观机理,利用 SRIM 模拟了 Cu^{2+} 离子注入两种材料的电子能量损失和核能量损失,并且模拟了两种光波导结构的折射率分布.模拟结果表明:熔融石英光波导的主要形成原因是离子注入表面的折射率大于其体材料的折射率,而石英晶体光波导的主要形成原因是离子射程末端的折射率小于其体材料的折射率.因此,在熔融石英光波导的形成中电子能量损失起主要作用,而在石英晶体光波导的形成中核能量损失起主要作用.

关键词:集成光学;光波导结构;离子注入;熔融石英;石英晶体
中图分类号:O439　　**文献标识码**:A　　**文章编号**:1004-4213(2017)04-0413001-7

Properties of Waveguide in Fused Silica and Quartz Crystal Fabricated by Cu^{2+} Ion Implantation

LIU Xiu-hong, HAN Hai-yan, ZHU Qiao-fen, HUANG Yan-bin, DONG Zhao
(*School of Mathematics & Physics, Hebei University of Engineering, Handan, Hebei* 056038, *China*)

Abstract: Planar waveguides were fabricated in fused silica and quartz crystal by Cu^{2+} ion implantation respectively. The guiding mode property was investigated in two types of waveguides by the prism-coupling method. The results indicate that an enhance-type waveguide formed in fused silica, while a barrier-type waveguide formed in quartz crystal by the same ion implantation. The anealing effects to the effective refractive indices of guiding modes in two types of waveguides were researched. The effective refractive indices of the guiding modes in fused silica decrease with the increase of annealing temperature. However, in quartz crystal the effective refractive indices of the guiding modes increase firstly and then decrease with the increase of annealing temperature. In order to investigate the formation mechanism of two kinds of waveguide, the distribution of the electronic and nuclear energy deposition in fused silica and quartz crystal were simulated using the SRIM code. In addition, the refractive index profiles of the types of waveguide were reconstructed. The simulation results show that in fused silica the main reason of the waveguide formation is that the refractive index in the near-surface region is larger than the substrate. However, in quartz crystal waveguide the major formation reason is that the refractive index at the end of ion track is less than the substrate region. Therefore, the electronic energy damage plays an important role for the formation of fused silica waveguide, while nuclear energy deposition is the dominant factor in the quartz crystal waveguide.

Foundation item: The Natural Science Foundation of Hebei Province (Nos. A2015402035, B2015402066), the Science and Technology Research Foundation of Hebei Education Department for Young Teachers in University (Nos. QN2014134, QN2016090, YQ2014013).
First author: LIU Xiu -hong (1983－), female, lecturer, Ph. D. degree, mainly focuses on waveguide and optofluidic device. Email: liuxiuhong@hebeu.edu.cn
Received: Dec. 16, 2016; **Accepted**: Feb. 9, 2017

Key words: Integrated optics; Waveguide; Implantation; Fused silica; Quartz crystal
OCIS Codes: 130.2790; 130.3120; 160.6030; 230.7390

0 Introduction

Fused silica is one of the earliest integrated optical materials because of low cost, low transmission loss, high coupling efficiency, good light transmission and easy integration[1]. It is widely used in precision casting industry, optical fiber communication, electronics industry, chemical industry, ceramics, and metallurgy industry[2-4]. It can be utilized as refractories and thermal insulation material[5-6]. Quartz crystal is an important electronic material owing to its strong piezoelectric effect, low thermal expansion coefficient, good mechanical properties, excellent frequency stability and frequency selective characteristic[7-8]. It can be produced to ideal sensor[9], filter, resonator[10-11], and microbalance[12-14]. Although the fused silica and quartz crystal have the same chemical composition, but their microstructure is different. Fused silica is amorphous, while quartz crystal is crystal structure.

Ion implantation is a unique method to produce optical waveguides in many optical materials[15-16]. There were several reports on waveguides in fused silica and quartz crystal by ion implantation[17-19]. However, to our knowledge, there has been no report on comparison between the two kinds of waveguide fabricated by the same method. Implantation of heavy ions has been proven to be a better strategy for waveguide fabrication due to the lower dose requirements. Considering that, we choose Cu^{2+} ion implantation in our experiment. In our work, we fabricated planar waveguides in fused silica and quartz crystal by the same ion implantation condition. And then, we investigated the formation mechanism by measuring guide mode properties of the two kinds of waveguides. In this paper, we mainly focus on clarifying the different formation mechanism of the waveguide between fused silica and quartz crystal by means of contracting the optical properties of two different types of waveguides.

1 Experimental details

The fused silica sample with size of 6 mm×8 mm×2 mm and the quartz crystal sample with size of 6 mm×5 mm×2 mm were cleaned and optically polished before Cu^{2+} ion implantation. One of the largest faces of these samples were implanted by 3 MeV Cu^{2+} ion in fluence of 5×10^{15} ions/cm^2 at room temperature using a 1.7 MV tandem accelerator at Peking University. To avoid channeling affects in quartz crystal, all the samples were tilted 7° off the beam direction. The schematic diagram of waveguide structure is shown in Fig. 1. After ion implantation, we carried out an annealing treatment using a furnace in open atmosphere to reduce damage and color centers caused by implantation. The temperature was increased in step and the annealing time was 1 h for each constant temperature. We performed the dark mode measurement of the two kinds of waveguide before and after annealing treatment using a prism coupler (Model 2010 Metricon, USA) at 633 nm and 1539 nm, respectively. We used the end-face coupling method to obtain the near-field optical intensity distributions for waveguides after annealed treatment, where light from a He - Ne laser (633 nm) was coupled into the waveguide by a 25× microscope objective. The output light was collected by another 25× microscope objective and detected by a CCD camera connected with a computer. To compare the range profile for 3 MeV Cu^{2+} ion implantation in fused silica and quartz crystal, we used the Stopping and Range of Ions Matter (SRIM) code[20] to simulate the process. The refractive index profile of the fused silica waveguide and quartz crystal waveguide were reconstructed by a FORTRAN program code based on the Reflectivity Calculation Method (RCM)[21].

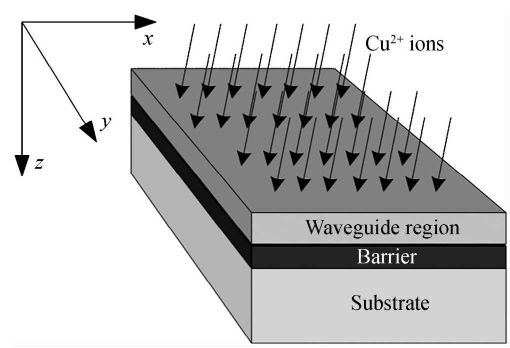

Fig. 1 Schematic diagram of waveguide structure

2 Results and discussion

Here, we used a prism coupler (Model 2010 Metricon, USA) with two lasers at fixed wavelengths of 633 nm and 1539 nm to measure the guiding modes of the fabricated waveguides. The guiding mode of the ion-implanted waveguide can be excited by incident light when the incident angle matches the guiding mode. Otherwise, the leaky mode will form in the ion-implanted waveguide. Fig. 2 is the dark mode spectrum at 633 nm and 1539 nm for fused silica planar waveguide before annealing. It shows the measured relative intensity of the TE (transverse electric) polarized light reflected from the prism versus the refractive index of the incident light for the fused silica planar waveguides. Generally speaking, for an ion-implanted waveguide, sharp dips in the intensity spectra mean guiding modes, while broader dips correspond to leaky modes[22-23]. Considering the amorphous structure of the fused silica, we have not given the guiding mode result for TM (transverse magnetic) polarized light in this paper. For comparison, we indicated the refractive index in the substrate by a dashed line in Fig. 2. As one can see in Fig. 2, there are two guiding modes at 633 nm, while one guiding mode at 1539 nm for TE polarized light. The effective refractive indices of TE modes are larger than that of fused silica virgin.

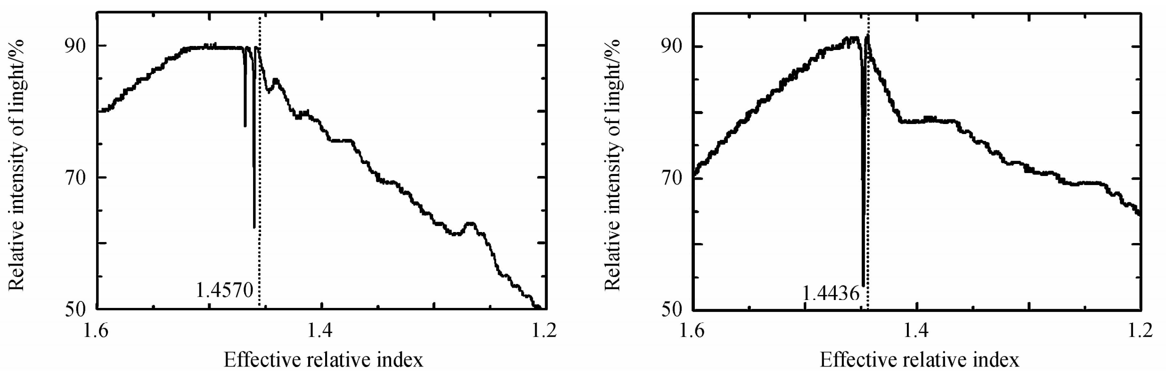

(a) The guiding modes in fused silica waveguide at 633 nm (b) The guiding modes in fused silica waveguide at 1539 nm

Fig. 2 Dark mode spectrum in fused silica waveguide

We also measured dark mode spectrum of the quartz crystal waveguide at the wavelength of 633 nm and 1539 nm, as is shown in Fig. 3. For comparison, we indicate the refractive index in the substrate by a dashed line in Fig. 3. There are three guiding modes at 633 nm, while two guiding modes at 1539 nm for the TE polarized light. The effective refractive indices of TE modes are smaller than that of quartz crystal virgin ($n = 1.5422$ at 633 nm, $n = 1.5270$ at 1539 nm). Comparing Fig. 2 and Fig. 3, we can see that different types of optical waveguide have formed in fused silica and quartz crystal under the same implantation condition.

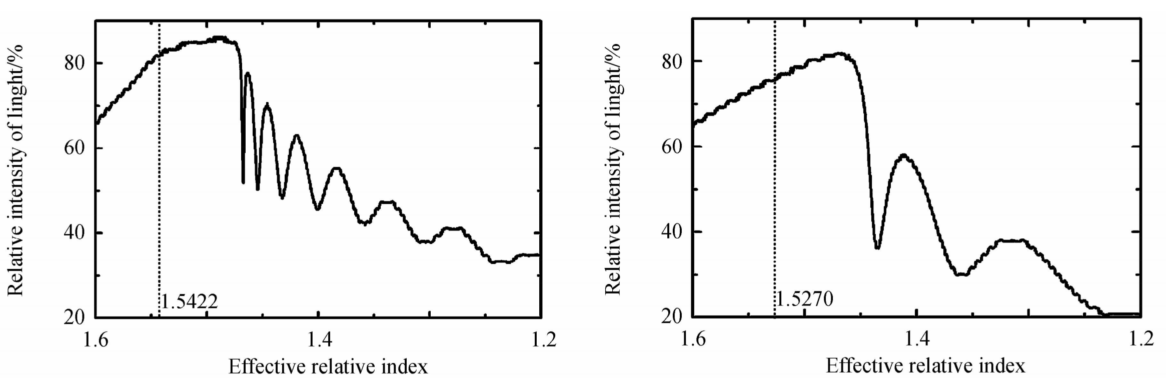

(a) The guiding modes in quartz crystal waveguide at 633 nm (b) The guiding modes in quartz crystal waveguide at 1539 nm

Fig. 3 Dark mode spectrum in quartz crystal waveguide

We simulated the Cu^{2+} ion implanted process in fused silica and quartz crystal using the Stopping and Range of Ions Matter (SRIM) code[20]. Fig. 4 shows the distribution of the electronic and nuclear energy deposition in fused silica and quartz crystal. The nuclear damage is concentrated at the end of the Cu^{2+} ion range, while the electronic damage takes place mainly during the trajectory of incident ions. A majority of the nuclear energy damage distibuted at the depth of 2.31 μm for fused silica, while 1.9 μm for quartz crystal. In quartz crystal, partial or completed amorphization of the lattice occurs as a result of nuclear damage at the end of the ion track, which is accompanied by a decrease in the refractive index. Such an index decrease acts as an optical barrier and a waveguide formed between air and the optical barrier.

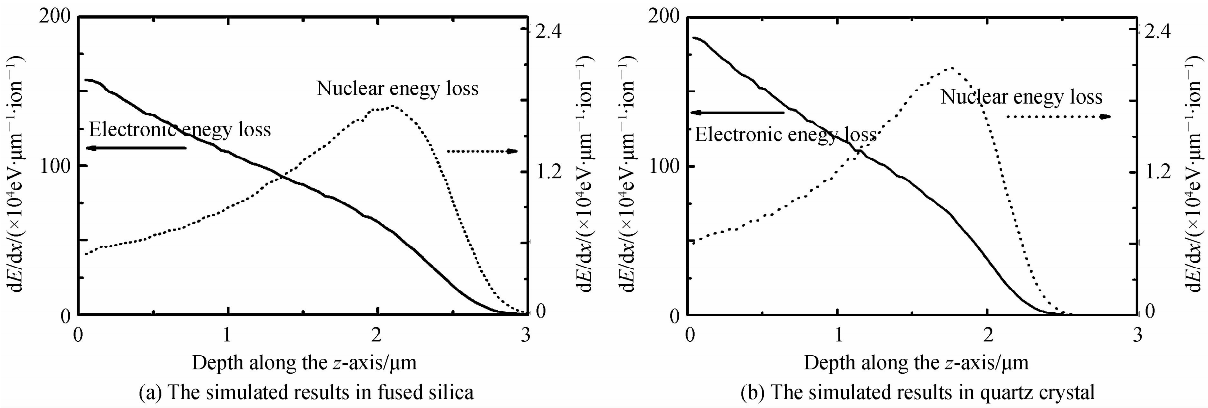

(a) The simulated results in fused silica

(b) The simulated results in quartz crystal

Fig. 4 Distribution of electronic enegry depositon and nuclear energy deposion of 3 MeV Cu^{2+} ion fused silica and quartz crystal by SRIM 2013.

The refractive index profile of two types of waveguides were reconstructed by using the RCM[21], as in shown in Fig. 5. An enhanced-type planar waveguide formed in fused silica, while a barrier-type waveguide formed in quartz crystal after Cu^{2+} ion implantation. Comparing Fig. 4(a) and Fig. 5(a), we know that in fused silica the electronic energy damage play an important role for the positive alternation of the refractive index occurred in the near-surface region, while nuclear collisions correlate to the negative alternation at the end of ion track[24]. From the results in Fig. 4(b) and Fig. 5(b), one can see that in the quartz crystal waveguide nuclear energy deposition is the dominant factor for the optical barrier with decreased refractive indices. This result is consistent with previous reports[25-26].

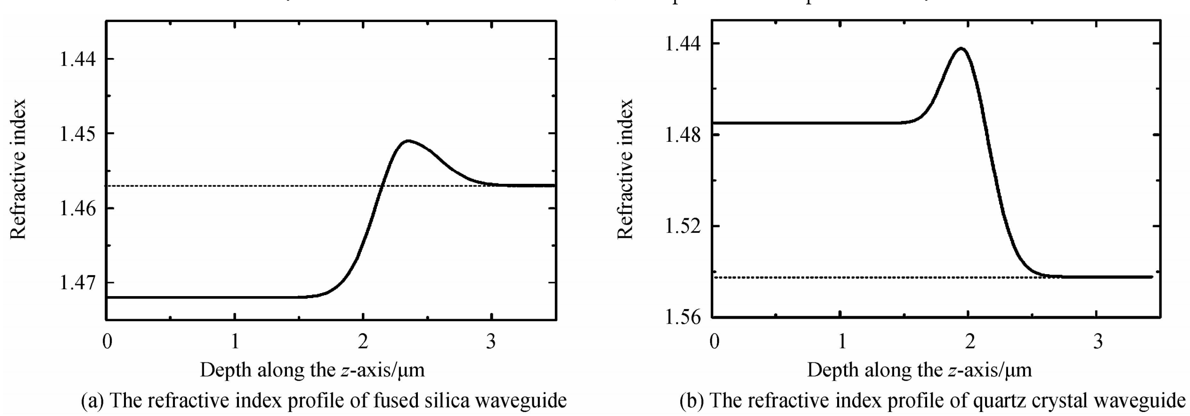

(a) The refractive index profile of fused silica waveguide

(b) The refractive index profile of quartz crystal waveguide

Fig. 5 Reconstructed refractive index profile of the planar waveguide

After ion implantation, we performed continuous annealing treatments in atmosphere for two kinds of waveguide (Table 1). After each annealing step, we measured the dark mode spectrum of the waveguide. The corresponding effective refractive indices of the TE_0 mode and TE_1 mode are shown in Fig. 6. We can see that the effective refractive indices of the guiding modes in fused silica decrease with each annealing treatment , owing to the recovery of damage in the waveguide region . However , in quartz crystal the effective refractive index of the TE_0 mode increase after annealed at 273℃ for one hour, and then decrease after annealed at 400℃ for one hour. The change of the effective refractive index of the TE_0 mode is related to re-crystallization of the amorphous structure in the waveguide region. The refractive index depends on the polarizability and

Table 1 Annealing treatment conditions for waveguides in fused silica and quartz crystal

Process	Fused silica	Quartz crystal
S_0	As implanted	As implanted
S_1	227℃ for 1 h	227℃ for 1 h
S_2	S_1+300℃ for 1 h	S_1+400℃ for 1 h
S_3	S_2+350℃ for 1 h	/

the atomic density in crystal[27]. The refractive index becomes smaller with the increase of the volume expansion, while becomes larger with the increase of polarizability. As the temperature rises, the volume and the polarizability will all increase. So the refractive index has a non-monotone variation as the temperature increase.

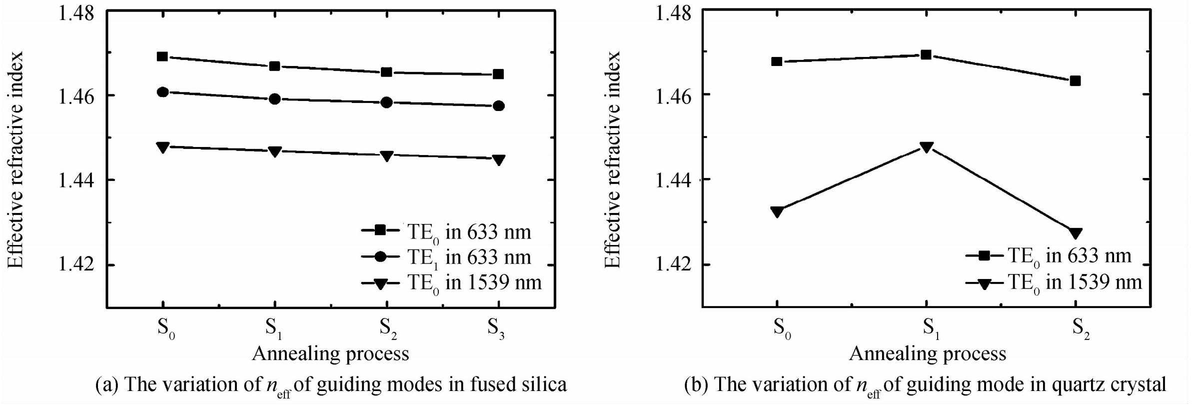

Fig. 6 The variation of the effective refractive index of guiding modes

We got the near-field intensity distribution of the TE polarized light through the fused silica waveguide after annealing at 300℃ for one hour. However, for quartz crystal waveguide we have obtatined the near-field intenstiy profile of the TE polarized light untill annealing at 400℃ for one hour. Quartz crystal need higher temprature to recover the damage. Fig. 7 is the near-field intensity distribution of the TE_0 mode in fused silica waveguide after annealing treatment under two-dimensional condition (2D) and three dimensional condition (3D). Correspondingly, Fig. 8 is the near-field intensity distribution of the TE_0 mode in quartz crystal waveguide after annealing treatment under 2D and 3D conditions. The results verify that the guiding mode is well confined in the waveguide. Comparing Fig. 7 and Fig. 8, we know that the enhanced-type planar waveguide perform better than the barrier-type waveguide.

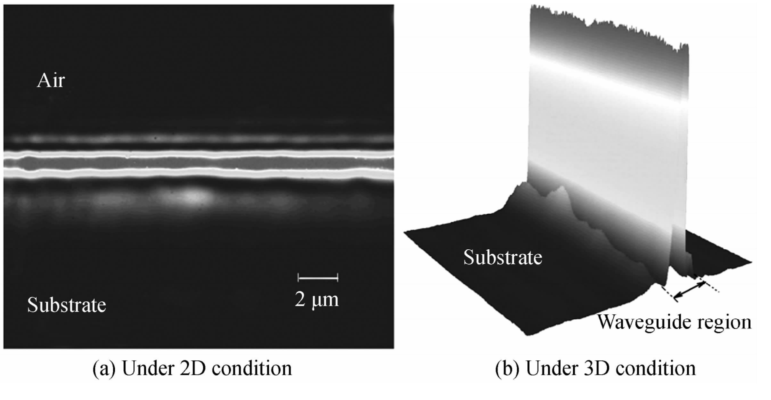

Fig. 7 Near-field light intensity distribution of the TE polarized light in the fused silica waveguide

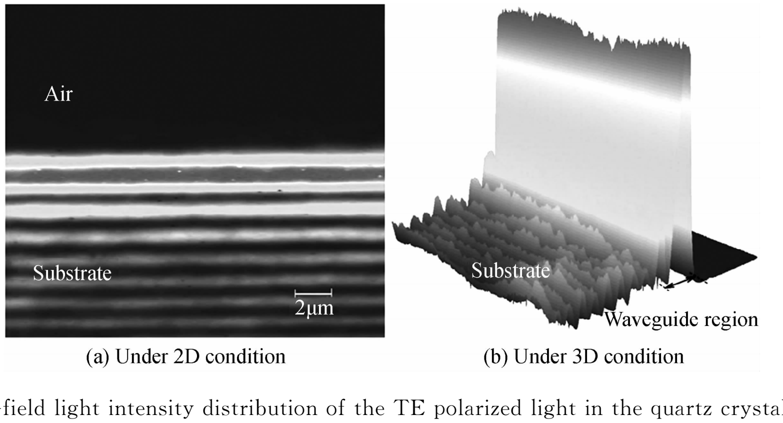

Fig. 8 Near-field light intensity distribution of the TE polarized light in the quartz crystal waveguide

3 Conclusion

we fabricated two kinds of planar waveguide in fused silica and quartz crystal by the same Cu^{2+} ion implantation. An enhance-type waveguide formed in fused silica, while a barrier-type waveguide formed in quartz crystal. The effective refractive indices of the guiding modes in the two kinds of waveguides present different behavior with annealing treatment. That is to say, microstructure is an important affect in the formation of optical waveguide.

References

[1] KARASINSKI P, TYSZKIEWICZ C, DOMANOWSKA A, *et al*. Low loss, long time stable sol - gel derived silica - titania waveguide films[J]. *Materials Letters*, 2015, **143**: 5-7.

[2] SHAO L Y, CANNING J, WANG T, *et al*. Viscosity of silica optical fibers characterized using regenerated gratings [J]. *Acta Materialia*, 2013, **61**(16): 6071-6081.

[3] GAO T Q, ZHAO Y, ZHOU G H, *et al*. Fabrication and characterization of three dimensional woven carbon fiber/silica ceramic matrix composites[J]. *Composites Part B: Engineering*, 2015, **77**: 122-128.

[4] SUN Z M, ZHOU C H, CAO H C, *et al*. Unified beam splitter of fused silica grating under the second Bragg incidence [J]. *Journal of the Optical Society of America A*, 2015, **32**(11):1952-1957.

[5] PILATE P, LARDOT V, CAMBIER F, *et al*. Contribution to the understanding of the high temperature behavior and of the compressive creep behavior of silica refractory materials[J]. *Journal of European Ceramic Society*, 2015, **35**(2): 813-822.

[6] LIAN T W, KONDO A, KOZAWA T, *et al*. Effect of fumed silica properties on the thermal insulation performance of fibrous compact[J]. *Ceramics International*, 2015, **41**(8): 9966-9971.

[7] VERISSIMO M, GOMES M, Assessment on the use of biodiesel in cold weather: pour point determination using a piezoelectric quartz crystal[J]. *Fuel*, 2011, **90**(90): 2315-2320.

[8] LI K W, WANG Z B, WANG L M, *et al*. 45° double-drive photoelastic modulation[J]. *Journal of the Optical Society of America A*, 2016, **33**(10): 2041-2046.

[9] KANG Q, SHENG R, LI Y L, *et al*. Real time monitor electroless plating of Ni - P film on quartz surface by an electrode-separated piezoelectric sensor[J]. *Sensors & Actuators B Chemical*, 2011, **157**(2): 533-539.

[10] LE G D, HELARY G, GINDRE M, *et al*. Monitoring cell adhesion processes on bioactive polymers with the quartz crystal resonator technique[J]. *Biomaterials*, 2005, **26**(19): 4197-4205

[11] WANG J, WANG Y, HU W K, *et al*. Huang, parallel finite element analysis of high frequency vibrations of quartz crystal resonators on Linux cluster[J]. *Acta Mechanica Solida Sinica*, 2008, **21**(6): 549-554.

[12] HABIBI N, PASTORINO L, RUGGIERO C, Functionalized biocompatible polyelectrolyte multilayers for drug delivery: In situ investigation of mechanical properties by dissipativequartz crystal microbalance[J]. *Materials Science & Enginerring C Materials for Biological Applications*, 2014, **35**(2): 15-20.

[13] HILLMAN A R, RYDER K S, ZALESKI C J, *et al*. Application of the combined electrochemical quartz crystal microbalance and probe beam deflection technique in deep eutectic solvents[J]. *Electrochimica Acta*, 2014, **135**(22): 42-51.

[14] VITTORIAS E, KAPPL M, BUTT H J, *et al*. Studying mechanical microcontacts of fine particles with the quartz crystal microbalance[J]. *Powder Technology*, 2010, **203**(3): 489-502.

[15] XIANG B X, WANG L, JIAO Y, *et al*. Low-loss optical waveguides preserving photoluminescence features in Pr^{3+}-doped yttrium orthosilicate crystal fabricated by ion implantation[J]. *Journal of Lightwave Technology*, 2015, **33** (11): 2263-2267.

[16] QIAO M, WANG T J, SONG H L, *et al*. Lattice damage and waveguide properties of medium- and high-energy C^{3+} ions-irradiated $LaAlO_3$ crystals[J]. *Applied Physics B*, 2017, **123**:19.

[17] CRESPILLO M L, GRAHAM J T, ZHANG Y, *et al*. In-situ luminescence monitoring of ion-induced damage evolution in SiO_2 and Al_2O_3[J]. *Journal of Luminescence*, 2016, **172**: 208-218.

[18] PLAKSIN O A, TAKEDA Y, KONO K, *et al*. Optical effects in silica glass during implantation of 60 keV Cu^- ions [J]. *Applied Surface Science*, 2005, **244**(1): 79-83.

[19] Ramírez-Espinoza C, Salazar D, Rangel-Rojo R, *et al*. Design of step-index optical waveguides by ion implantation[J]. *Journal of Lightwave Technology*, 2015, **33**(14): 3052-3059.

[20] ZIEGLERJ F. "Computer code", SRIM2013[EB/OL]. [2016-12-16]. http://www.srim.org.

[21] CHANDLER P J, LAMA F L, A new approach to the determination of planar waveguide profiles by means of a non-stationary mode index calculation[J]. *Journal of Modern Optics*, 1986, **33**(2): 127-143.

[22] WANG T J, ZHOU Y F, YU X F, *et al*. Optical waveguide properties of $Ca_{0.4}Ba_{0.6}Nb_2O_6$, crystal formed by oxygen ion irradiation[J]. *Nuclear Instruments & Methods in Physics Research*, 2015, **354**: 187-191.

[23] TAN Y, CHEN F, WANG L, *et al*. Carbon ion-implanted optical waveguides in Nd:$YLiF_4$ crystal: Refractive index profiles and thermal stability[J]. *Nuclear Instruments and Methods in Physics Research B*, 2007, **260**(2): 567-570.

[24] BENTINI G G, BIANCONI M, CHIARINI M, *et al*. Effect of low dose high energy O^{3+} implantationon refractive index and linear electro-optic properties in X-cut $LiNbO_3$: planaroptical waveguide formation and characterization[J]. *Journal of Applied Physics*, 2002, **92**(11): 6477-6483.

[25] LIU X H, ZHAO J H, ZHANG S M, *et al*. Damage behaviors in Nd:YVO_4 by multi-energy proton implantation[J]. *Nuclear Instruments & Methods in Physics Research*, 2012, **286**(9): 213 - 217.

[26] MANZANO-Santamaría J, OLIVARES J, RIVERA A, *et al*. Electronic damage in quartz (c-SiO_2) by MeV ion irradiations: Potentiality for optical waveguiding applications[J]. *Nuclear Instruments & Methods in Physics Research*, 2012, **272**(3): 271-274.

[27] JIANG Y, WANG K M, WANG X L, *et al*. Model of refractive-index changes in lithium niobate waveguides fabricated by ion implantation[J]. *Physical Review B*, 2007, **75**: 195101.